

Grain-size effect on structure and phase transformations for barium titanate

M. H. Frey and D. A. Payne

Department of Materials Science and Engineering, Seitz Materials Research Laboratory, and Beckman Institute, University of Illinois at Urbana-Champaign, Urbana, Illinois 61801

(Received 23 February 1996)

We report the results of an investigation into the grain-size dependence of lattice structure for barium titanate (BaTiO_3) ceramics prepared by a sol-gel method. Raman and infrared spectroscopy, x-ray diffraction, and differential scanning calorimetry were used in combination with electron microscopy to study the evolution of lattice structure and phase transformation behavior with heat treatment and grain growth from the nano scale to the micron scale for BaTiO_3 polycrystals. Raman spectroscopy and optical second-harmonic-generation measurements indicated the onset of local room-temperature acentric crystal symmetry with heat treatment and crystallite growth, well before the observation of any tetragonal structure by x-ray diffraction. Analysis of the room-temperature Raman spectra for ultrafine grain (grain size $< 0.1 \mu\text{m}$) polycrystals suggested that a locally orthorhombic structure preceded the globally tetragonal form with grain growth. In support of this observation, differential scanning calorimetry suggested the orthorhombic-tetragonal phase transformation shifts up through room temperature with decreasing grain size. Hot-stage transmission electron microscopy studies revealed that fine grain (grain size $\approx 0.1 \mu\text{m}$) ceramics, which showed a thermal anomaly associated with the cubic-tetragonal phase transformation, were untwinned at room temperature, as well as on cycling through the normal Curie temperature, suggesting a single-domain state for individual grains. The findings are discussed in light of a number of possible causes, including the presence of processing-related hydroxyl defects and the effect of elastic constraints on phase transformation behavior for BaTiO_3 grains in a polycrystalline microstructure. [S0163-1829(96)05426-4]

I. INTRODUCTION

In this paper we report results for an experimental investigation of the grain-size effect on structure and properties for barium titanate (BaTiO_3) ceramics. Of current concern is the extent to which bulk physical properties can be considered for the design of miniaturized thin-layer devices from the micron scale to the nano scale. As ferroelectric ceramics find increasing processibility as active elements in micro-electronic devices, there is sustained interest in size-dependent characteristics. The structure and properties of thin-layer ferroelectrics, integrated on semiconductor substrates for example, are well known to exhibit a number of deviations from those of bulk ceramics or single crystals. The most often cited of such departures is referred to as the size effect for BaTiO_3 . We consider a number of observations and viewpoints related to this widely reported subject, particularly with regard to chemically prepared materials. Then, we report our own findings for a grain-size effect on lattice structure and phase transformation behavior for polycrystalline BaTiO_3 .

A. Size effects in ferroelectric ceramics

Over 40 years ago a grain-size effect was reported by Kniepkamp and Heywang for the dielectric properties of polycrystalline BaTiO_3 .¹ It was generally recognized that as the grain size was reduced to the micron level, the dielectric constant at room temperature increased, and that the temperature dependence of the dielectric constant was modified significantly below the Curie temperature (T_C). It is well known that for larger grain materials (grain size $> 1 \mu\text{m}$),

the cubic-tetragonal transformation that occurs on cooling (130°C) drives the formation of a polydomain subgrain structure to minimize electrostatic and elastic energies in the polar anisotropic state. The polysynthetic twinning that takes place serves largely to relieve stresses which would otherwise be present throughout the transformed body. That is, individual grains in the transformed microstructure of a large grain polycrystal are comprised of a multitude of structural variants, bounded by domain walls of 90° and 180° types in the tetragonal state. Thus, large grain centers are usually fully transformed and essentially unstressed. The dielectric response of such a material is readily rationalized in terms of an orientational average of values for the anisotropic dielectric constant which characterizes a single domain of tetragonal BaTiO_3 .²

Within several years of its discovery, it was observed that polycrystalline BaTiO_3 exhibited an enhanced dielectric response for ceramic specimens prepared with a grain size as small as $1 \mu\text{m}$.¹ The increase in dielectric constant is now understood in terms of the twinning behavior of polycrystals with decreasing grain size. Despite the ability of the twinning mechanism to reduce the bulk strain energy that would be present after a homogeneous structural transformation occurred, stress does still reside near grain boundaries, even for large grain ceramics. Minimization of the residual strain energy ultimately contributes to the resulting twin structure.³ Arlt *et al.* showed that as the grain size of BaTiO_3 was reduced, the density of twins required to substantially relieve the transformation stress within the grain interior, and minimize the residual stress near grain boundaries, increased.⁴ With regard to the enhanced dielectric constant of submicron BaTiO_3 , which was anomalously higher than values ac-

cepted for single crystal specimens, it was discovered that very fine grain polycrystals were substantially untwinned. Now, it is explained that for these fine grain (grain size $< 1.0 \mu\text{m}$) materials with decreasing grain size, the increasing cumulative domain-wall energy associated with the formation of a polydomain subgrain structure becomes too costly compared to the achievable volume free energy change for the transformation.⁵ Thus, without twinning, a condition of grain clamping develops, whereby the transformation strain is suppressed to some extent. Buessen, Cross, and Goswami explained how the resulting microstructural stresses could lead to an enhanced dielectric constant for fine grain BaTiO_3 .⁶ Thus, it is well known that grain size can have a dramatic influence on crystal structure and properties for ferroelectric ceramics.

In addition to the work just described on microstructure-property relations for submicron polycrystalline BaTiO_3 , there has long been an interest in structural changes that take place upon further grain size reduction to the nano scale, driven by a need to better understand the properties of integrated thin-layer ferroelectrics.⁷ Unfortunately, few reports have been put forth which lead to a solid understanding of size-dependent phenomena for polycrystalline BaTiO_3 at such a small grain size and scale. Rather, many authors have restricted their work to investigations of small free particles or small crystallites assembled into some poorly characterized state of agglomeration. Numerous studies have been reported where BaTiO_3 was synthesized by some chemical route, and x-ray diffraction (XRD) was used to conclude that a room-temperature pseudocubic structure preceded the stable room-temperature tetragonal form with heat treatment to higher temperatures and with particle growth.^{8–12} The most often cited of such studies is that of Uchino, Sadanaga, and Hirose where temperature-dependent XRD studies suggested that with decreasing particle size, T_C was shifted downward through room temperature, eventually tending toward 0 K at some critical particle size.⁹ The authors combined various means of crystal size determination and XRD data to place the critical size at $0.12 \mu\text{m}$. They suggested that the cubic crystal structure, which characterized the small chemically prepared particles ($< 0.12 \mu\text{m}$) of BaTiO_3 at room temperature, was no different from the prototypic cubic structure which characterizes a large single crystal above T_C .

This idea of a critical size for ferroelectricity has long existed, and has been applied to other materials like PbTiO_3 , and to BaTiO_3 in other forms involving small crystal sizes, including polycrystalline ceramics.^{13–16} The data and conclusions presented in this paper are strongly related to the concept of a critical size for ferroelectricity. In particular, it will be shown that the view of a critical size, as it has been defined and determined in the works just cited, may be somewhat narrow. The presently reported research has revealed that, for sol-gel processed BaTiO_3 polycrystals, the normal cubic-tetragonal phase transformation does not simply shift downward through room temperature and on to 0 K with crystallite size reduction. Specifically, the cubic-tetragonal transformation shifts only slightly downward with grain-size reduction before being substantially suppressed. Concurrently, the orthorhombic-tetragonal transformation shifts upward slightly before experiencing the same suppression. That

is, a more complex evolution of subtle changes in structure and phase transformation behavior takes place. Also, it will be emphasized that there exists not a single size effect for BaTiO_3 . Rather, there are several reasons why crystal size, in the cases of free particles and crystallites in a bulk ceramic or a thin film, should influence the structure of BaTiO_3 .

The more widely considered possible causes for the apparent cubic and nonferroelectric structure of ultrafine BaTiO_3 are the following: depolarization effects, the absence of long-range cooperative interactions, structural defects, and elastic constraints. Depolarization fields result from an uncompensated spontaneous polarization for a ferroelectric material.¹⁷ When a ferroelectric material spontaneously polarizes, the free surface accumulates compensating charge from the environment, from an external circuit, and/or through internal transport of charged defects. After doing so, the full spontaneous polarization can be realized. If for some reason a spontaneous polarization would not be compensated by charge, the consequence of the necessary boundary condition of zero polarization at the free surface would be an internal electric field oriented opposite to the polarization (\mathbf{P}) itself. Stated differently, the gradient in polarization from the bulk to the surface would become a source for a depolarization field (\mathbf{E}), where L is a geometric factor, and ϵ and ϵ_0 are the relative permittivity and permittivity of free space, respectively:¹⁷

$$\mathbf{E} = -\frac{L}{\epsilon_0} \mathbf{P}, \quad (1)$$

$$W_E = \frac{1}{2} \int \frac{\epsilon}{\epsilon_0} L^2 P^2 dV. \quad (2)$$

In the absence of compensating charge, the depolarization field can, in principle, become sufficiently strong that its energy (W_E) would exceed the free energy reduction for the ferroelectric transition for a given volume (V) of material. Thus, the ferroelectric phase can become thermodynamically unstable. Of course, this phenomenon is never seen in bulk ferroelectrics, because of the numerous mechanisms for compensation. In addition to surface charge compensation, head-to-tail arrangements for ferroelectric domains reflects a mechanism to minimize the depolarization energy. The present issue relates to the possibility that the depolarization field might play a substantial role in size-related phenomena for BaTiO_3 .

The works of Uchino, Sadanaga, and Hirose and Batra and co-workers suggest the possibility of depolarization being a key influence in size-related phenomena for BaTiO_3 .^{9,18–20} The often cited work of Batra and co-workers involves a uniaxial ferroelectric sandwiched between semiconductor layers. The authors considered the spontaneous polarization (P_s) and ferroelectric transition temperature for triglycinesulfate thin films under the conditions of decreasing ferroelectric layer thickness and/or semiconductor carrier density. They showed theoretically that for the sandwiched arrangement described above, decreasing the thickness of the monodomain thin layer with its polarization oriented normal to the film plane, should lead to reduced polarizations and ferroelectric transition temperatures. Experimentally, the destabilization of the ferroelectric phase was demonstrated us-

ing high-electric field measurements made with semiconducting electrodes of various carrier density. That is, the effect of the depolarization field to destabilize a polar phase was demonstrated. Recall that in the work of Uchino, Sandanaga, and Hirose, the ferroelectric transition temperature of BaTiO_3 , as revealed by XRD, appeared to shift toward 0 K with particle size reduction. The obvious difference in these studies lies in the boundary conditions which exist for the different materials. The depolarization effect in the work of Batra *et al.* was easily controlled and addressed because of the semiconductor layers on each side of the ferroelectric layer. For the particles in the work of Uchino, Sandanaga, and Hirose, no such clear boundary conditions existed. The outstanding question is the following: In the presence of a driving force for the ferroelectric transition, would very fine ($<0.1 \mu\text{m}$) single-crystal particles of BaTiO_3 suffer the overwhelming strength of the depolarization field, or would they find a mechanism for its avoidance, be it the accumulation of compensating charge, the formation of a polydomain structure, or both? The topic of depolarization will be taken up again with regard to the results presented in this paper for polycrystalline material.

A second view of the cause of size effects in BaTiO_3 relates to the driving force itself for the ferroelectric transition. It clearly differs from the proposed effects of the depolarization field in this way. Proponents of the second view suggest that with decreasing size, the long-range interactions which support the development of a homogeneous spontaneous polarization are too significantly lessened even to drive the transformation.^{21,22} The length factors used to describe the interaction between polar units in ferroelectric materials are the correlation lengths parallel and perpendicular to the polarization vector. Lines and Glass state that correlation lengths parallel and perpendicular to the polar direction range from 10–50 nm and 1–2 nm, respectively.¹⁷ Based on the values cited above, and as Lines and Glass explain, one might expect significant effects on phase stability when crystallite dimensions are reduced into these ranges. Interestingly, however, Boyer showed through molecular-dynamics simulations that ferroelectric clusters on this short length scale should be stable for a hypothetical perovskite halide ferroelectric, and commented on the possibility that similar behavior could be expected for perovskite-structured oxides like BaTiO_3 .²³ Of course, other factors may come into play more strongly with size reduction long before the effect of reduced long-range correlations operates. These might include the depolarization field or either of the next two possible influences.

A third view, particularly related to the commonly observed XRD-cubic structure for chemically prepared BaTiO_3 , relates to defects which can result from processing. It is well known that hydroxyl ions can reside as defects on oxygen sites within BaTiO_3 , and the resulting charged defects are probably compensated for by cation vacancies.^{24,25} Several spectroscopic studies have been carried out to characterize this defect.^{26–28} As a result, a number of narrowly spaced infrared absorption bands in the 3450–3550 cm^{-1} range have been assigned to the OH^- stretching mode for hydroxyl ions of various orientations in the unit cell of tetragonal BaTiO_3 . Several authors have reported that infrared spectra for hydrothermally prepared BaTiO_3 powders can be

interpreted in terms of the presence of internal hydroxyls.^{10,29,30} The proposal has been that such a high concentration of charged point defects might upset the long-range polar ordering which drives the cubic-tetragonal structural transformation on cooling. That is, the apparent cubic structure of fine chemically prepared BaTiO_3 may result from an extremely high defect concentration, rather than a finite-size effect. Along with this view, the possibility that the charged defects might serve to stabilize polar microdomains in chemically prepared ferroelectric specimens of small crystallite size should also be considered.

For fine hydrothermally prepared BaTiO_3 powders, other authors have attempted to separate the effects of hydroxyl defects and crystallite size on lattice structure. Hennings and Schreinemacher clearly showed that the development of a room-temperature global tetragonal structure with heat treatment for BaTiO_3 particles of 0.2 μm diameter, and prepared under hydrothermal conditions from acetate precursors, was associated with the elimination of hydroxyl defects, and not with particle growth.¹⁰ In contrast, Begg, Vance, and Nowotny concluded for hydrothermal powders prepared from $\text{Ba}(\text{OH})_2$ and hydrolyzed titanium alkoxide that the release of water from the particles on heat treatment was not at all associated with the development of a tetragonal distortion observable by XRD.¹¹ In the present work, we address this issue for alkoxide gel-processed, polycrystalline BaTiO_3 . An often overlooked characteristic of inorganic materials prepared in solution by polymeric sol-gel processing, under conditions of high hydrolysis content, is the enormous presence of bound hydroxyl groups. In the BaTiO_3 synthesized by crystallization of such gel precursors, the inclusion of hydroxyls within the perovskite structure should be very likely. The possible impact of such defects on the structural aspects previously assumed to result from crystallite size alone should be considered. We have sought to assess the possible role of hydroxyl defects on any apparent size effects for sol-gel processed BaTiO_3 . To this end, analyses of the presence, and then liberation, of the hydroxyl defects for BaTiO_3 processed from alkoxide-derived polymeric gels were combined with lattice structure and grain-size investigations.

Finally, the possible effects of elastic constraints on the ferroelectric transformation of ultrafine BaTiO_3 must not be overlooked. Recall that it is the elastic constraint which is believed to cause such strong dependences of domain structure and dielectric properties on grain size for ceramic specimens of grain size in the range of 0.5–1.0 μm . Specifically, it was already stated that BaTiO_3 ceramics of submicron grain size become substantially untwinned as crystallite size is reduced. This is a result of the ever-increasing energetic cost of a domain structure whose size scales positively with the square root of the grain size itself.⁵ It was explained that in this case, a condition of grain clamping must develop, whereby individual grains are unable to develop their full transformation strain, even if the driving force should exist. It is reasonable to suggest that XRD measurements on such specimens would reveal a structure tending toward cubic symmetry with crystallite size reduction. This possibility will be considered seriously in interpreting the data of this report.

The phenomenology and possible causes for the anomalous structure characteristics classified within the general

subject of size effects in BaTiO_3 have been presented. The most distinctive structural feature of ultrafine BaTiO_3 of various forms is its tendency to exhibit a cubic-type structure when examined by XRD. Several possible causes for this observation were described. All of them are reasonable, and yet distinctly different. The present work attempts not to identify some type of single critical size for BaTiO_3 . Likewise, it attempts not to arrive at a single cause for all phenomena related to crystal size for ferroelectric ceramics. Rather, the phenomenology of size effects on structure and phase transformations in ultrafine grain sol-gel processed polycrystals is reported. Results for this particular processing method are discussed thoughtfully in light of all the views just presented for size effects in BaTiO_3 .

B. Characterization of structure for BaTiO_3

It is important to appreciate the length scales probed by instruments for structure analysis. The most common technique for crystal structure evaluation of BaTiO_3 has been XRD. Because XRD is a technique which relies on coherent scattering from many unit cells, and in a spatially time-averaged fashion, it is not sensitive to subtle structure characteristics which exist for small crystal regions. In the case of BaTiO_3 experiencing its various phase transitions, diffraction peaks can shift and be present with separations less than 0.1° on the 2θ scale. At the same time, finite coherently diffracting domain-size effects can lead to increased peak breadths on the order of a full degree or more for regions with size less than 100 \AA .³¹ Thus, XRD will not readily be able to reveal very subtle unit-cell distortions which occur for microdomains sized far less than 100 \AA , for example. Therefore, it is reported here that XRD was used to probe global structure for BaTiO_3 crystallites of decreasing size. The structure suggested by XRD measurements will be taken to reflect the highest symmetry which could be expected to describe large crystal volumes, which might span numerous defects or uniformly distorted microdomains, sampled simultaneously. However, there are other techniques which are better suited to probe local structure and subtle symmetry changes. In this report, we emphasize the combination of XRD and Raman scattering for this type of length scale discrimination. Descriptions of Raman selectivity in terms of crystal symmetry for perovskites can be found.³² Briefly, based on selection rules, all of the optic modes of cubic perovskite-type materials should be Raman inactive. In contrast, all of these modes should be Raman active for the polar tetragonal structure. Raman activity also characterizes the optic modes of the polar orthorhombic and rhombohedral forms. Of course, the exact energetics and symmetries of these modes for the different phases vary. For BaTiO_3 specifically, reliable temperature-dependent Raman-scattering data has been recorded for large single-crystal samples, revealing the spectra which are characteristic of the different polymorphs.³³ Thus, Raman scattering can be used to probe crystal structure to some extent. And, the length scale probed is reduced essentially to that of individual unit cells.

Other authors have carried out studies of varying completeness where XRD and Raman-scattering results were compared for chemically prepared BaTiO_3 . Busca *et al.* reported, for hydrothermally prepared BaTiO_3 , a cubic crystal

structure determined by XRD, the presence of internal hydrogen defects detectable by infrared spectroscopy, and Raman activity that the authors ascribed to a tetragonal crystallographic distortion of the unit cell.²⁹ The combination of these data implied that structure at the local level was not of the high symmetry suggested by XRD measurements alone. However, a question remained about which of the following was true; (i) that the cubic structure revealed by XRD was a result of defects disrupting long-range ordering processes of the ferroelectric transformation; or (ii) that the defects were actually necessary to stabilize the polar structure on short length scales, giving rise to Raman activity? Schlag and Eicke reported similar XRD and Raman-scattering results for sol-gel processed BaTiO_3 .³⁴ Schlag *et al.* described the materials of that study as nanocrystalline particles.³⁵ As Busca *et al.* did, these authors also interpreted their data to suggest that a local tetragonal distortion characterized the ultrafine materials which appeared cubic to XRD. We should emphasize that, in the research described here, we have not simply repeated the work of these previous authors. Rather, we have combined structure analyses by both XRD and Raman scattering with hydroxyl defect evaluation by infrared spectroscopy, along with results of thermal analysis and microstructure observation by electron microscopy, to construct a substantially more complete characterization of the evolution of lattice structure with heat treatment for sol-gel processed BaTiO_3 . In addition, measurements of the optical second-harmonic-generation (SHG) intensity provided information related to the magnitude of acentric distortions for ultrafine materials. That is, as Lines and Glass pointed out, the first-order nonlinear optical coefficient of tetragonal BaTiO_3 varies linearly with the spontaneous polarization.¹⁷ The SHG intensity is reported in the present paper to reflect, to some degree, the magnitude of acentric distortions for ultrafine BaTiO_3 , keeping in mind the effect of crystal size itself on SHG intensity (*viz.*, phase matching).

II. EXPERIMENTAL

Nanocrystalline BaTiO_3 materials were prepared from alkoxide gel precursors, as reported previously for our work.^{36,37} Crystallized xerogels were ground lightly in a mortar and pestle to give polycrystalline pieces ($10\text{--}50 \mu\text{m}$) for higher temperature heat treatment and characterization. Thermal treatments were carried out by heating the dried product on zirconia trays in air at $10^\circ\text{C}/\text{min}$ to various temperatures from 300 to 1350°C , with holding at temperature for 1 h before furnace cooling. The aggregates were evaluated for residual carbon content by combustion analysis. Powder XRD (Rigaku D-Max III) was used to monitor the room-temperature global structural transition from apparent cubic to tetragonal symmetry. Raman spectra were recorded using the 514 nm line of an Ar^+ laser by focusing a 150 mW beam to about 1 mm onto filled capillary tubes. Data were collected and analyzed for the unpolarized radiation scattered at 90° with a triple monochromator (SPEX) and CCD camera. Measurements of the optical SHG intensity for specimens spread onto microscope slides, as suggested by Kurtz and Perry, were carried out using the 1064 nm line of a pulsed Nd:YAG laser.³⁸ The incident beam wavelength was filtered from the frequency-doubled light,

and the 532 nm intensity was determined. Diffuse reflectance infrared (IR) fourier transform spectroscopy (Nicolet 550) was carried out for each of the thermally processed samples. 15 mg of each specimen was added to 285 mg of KBr powder and ground in a mortar and pestle to give a fine mixture. Differential scanning calorimetry (DSC) measurements were made with the use of a liquid-nitrogen cooling accessory (TA Instruments MDSC 2920). The dependence of phase transformation behavior on grain size was investigated for 15–20 mg specimens. Values for the enthalpy of transition were determined for the tetragonal-cubic transformation and compared with measured and reported values for single crystals. Microstructures were observed for the sintered xerogel-derived pieces by high-resolution scanning electron microscopy (SEM, Hitachi S-800), and the grain sizes were determined for a number of processing conditions. Hot-stage transmission electron microscopy (TEM, Philips 420) studies were carried out on thinned specimens to evaluate the grain-size-dependent twinning behavior associated with any phase transition.

III. RESULTS AND DISCUSSION

We report now the evolution with heat treatment and grain growth of lattice hydroxyl defects and the room-temperature lattice structure, as determined by IR spectroscopy and by XRD and Raman scattering, respectively. Optical SHG measurements provide semiquantitative information on the magnitude of acentric distortions in ultrafine materials. Hot-stage TEM and DSC measurements give information on grain-size-dependent phase transformation behavior for BaTiO₃, and support conclusions drawn from Raman-scattering experiments about subtle changes in room-temperature local crystal symmetry.

A. Global structure vs local symmetry

The room-temperature transition from globally cubic to tetragonal symmetry, commonly observed for chemically prepared BaTiO₃ with increasing processing temperature, is demonstrated by the gradual splitting of the pseudocubic {200} into tetragonal (200) and (002) reflections in the XRD data of Fig. 1. A slight long-range tetragonal lattice distortion first starts to appear in materials heat treated at 1000 °C. Higher temperatures (1350 °C) are necessary to develop the net 1% *c*-axis cell elongation normally associated with the ferroelectric transition. As mentioned previously, many authors have analyzed, in considerable detail, XRD data taken from material undergoing this evolution in lattice structure. Again, Uchino, Sandanaga, and Hirose described a simple continuous decrease in *T_C* through room temperature for single-crystal particles of decreasing size.⁹ Takeuchi *et al.* looked closely at the (212), (102), and (103) reflections and proposed the coexistence of cubic surface layers and tetragonal grain cores, and the occurrence of changes in their proportions with heat treatment and particle growth.³⁹ Leonard and Safari examined the (222) reflection and decided that, for a particular commercially available hydrothermal BaTiO₃ powder, a coexistence of discretely different phases may exist, contrary to what one would conclude by looking only at the {200} reflection(s).⁴⁰ Arlt, Hennings, and deWith, based on analysis of the {400} reflections, reported a change

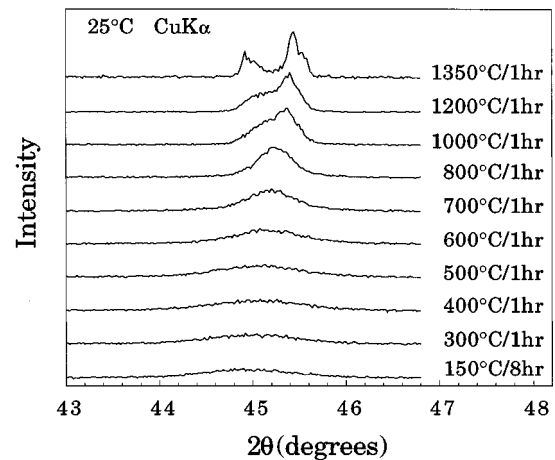


FIG. 1. Powder x-ray-diffraction data for the {200} reflections of BaTiO₃ crystallized initially at 150 °C and then processed to increasing temperature.

at room temperature from tetragonal to orthorhombic structure with decreasing grain size below 0.5 μm for BaTiO₃ ceramics.⁴ We present the data in Fig. 1 as a background for the analysis of spectroscopic and microscopic data. Figure 2 illustrates the evolution of the room-temperature pseudocubic and tetragonal lattice parameters with heat treatment, based only on the XRD {200} data. Clearly, the room-temperature lattice parameter contracted with increasing heat treatment temperature before any global symmetry change could be detected by XRD, as has been reported by others for chemically prepared BaTiO₃.^{8,10}

Figure 3 gives SEM photomicrographs for three of the heat treatment conditions, particularly 800, 1000, and 1200 °C. They were recorded for grain size determination for samples undergoing the transition as revealed by XRD. The samples are characterized by 0.035, 0.1, and 0.4 μm grain size, respectively. Thus, 0.035 μm ceramic BaTiO₃ appears by XRD to be characterized by cubic symmetry, while grain growth to 0.1 μm and beyond leads to slight lattice distortion readily detectable by XRD. Local symmetry, probed by Raman scattering, for these and other samples is next presented.

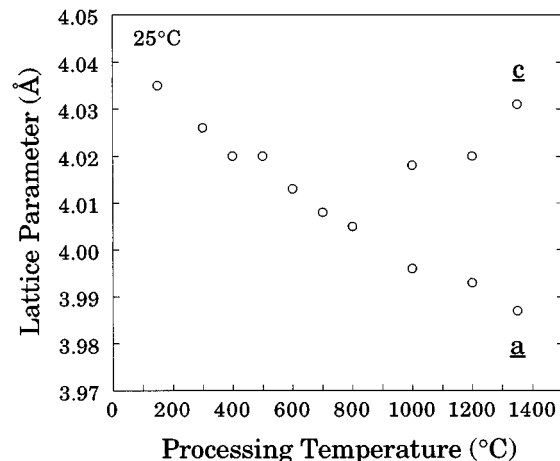


FIG. 2. Lattice parameters determined from the {200} XRD data, and representing the room-temperature cubic-to-tetragonal structural transition with increasing processing temperature.

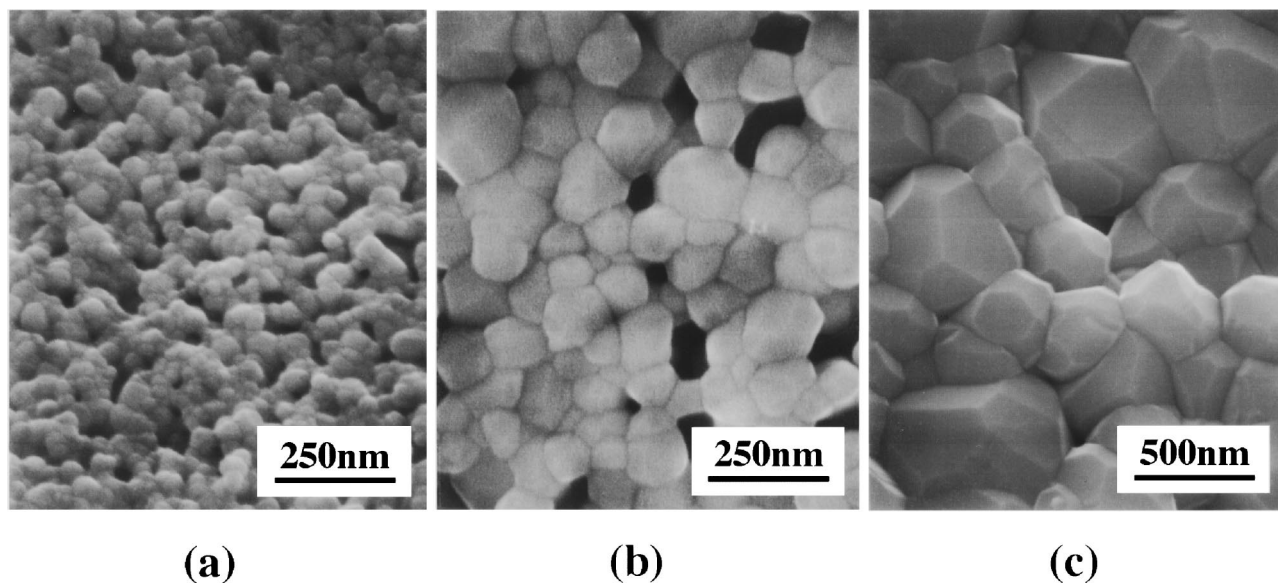


FIG. 3. SEM photomicrographs illustrating the grain growth with increasing heat-treatment temperature for sintered xerogel pieces; (a) 800 °C, (b) 1000 °C, (c) 1200 °C.

Figure 4 gives Raman spectra for a number of the specimens heat treated under different conditions. Peak positions observed for each of the spectra are summarized in Table I along with the results for carbon analysis and XRD observations. A small amount of residual carbonate could be identified for specimens processed below 700 °C, as evidenced by the peak centered at 1060 cm^{-1} in the Raman spectra.⁴¹ This finding is in agreement with transmission IR data that we have reported previously.³⁶ The shoulder located near 805 cm^{-1} for the same specimens is as yet unassigned. It appears not to be attributable to BaCO_3 , any phase of BaTiO_3 , the rutile or anatase forms of TiO_2 , or any other known phase in the BaO-TiO_2 system.^{33,42-44} The Raman-scattering data demonstrate the presence of acentric local structure for sol-gel processed BaTiO_3 of apparent cubic structure to XRD. Figure 4 gives Raman spectra similar to single-crystal data recorded at room temperature. However, the present data are for polycrystalline aggregates, many of which are cubic to

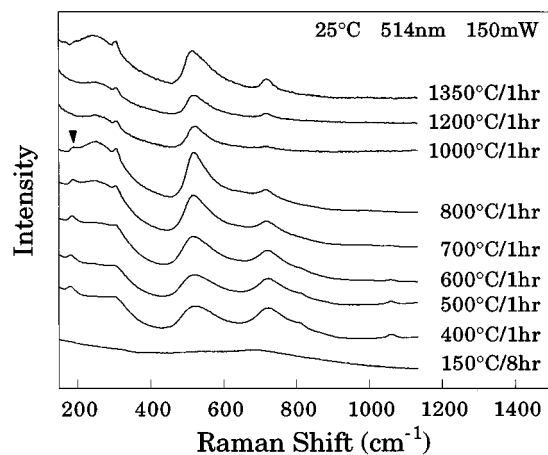


FIG. 4. Raman spectra for polycrystalline BaTiO_3 processed with increasing temperature from xerogel precursors.

XRD. Clear Raman peaks were not detected for as-dried and initially crystallized material (150 °C).

Robins *et al.* reported Raman spectra for a number of BaTiO_3 thin films prepared by metal-organic chemical-vapor deposition.⁴⁵ The authors were careful to point out that the broader features in the Raman spectrum of tetragonal BaTiO_3 centered near 250 and 515 cm^{-1} have been shown to persist strongly well above T_C , even in relatively pure single crystals and despite a violation of Raman selection rules.⁴⁶ This makes these peaks inappropriate for the conclusion that a structure which is in any way different from the cubic form above T_C exists. This Raman-scattering behavior may result from the presence of impurities or dynamic polar domains above T_C , or the occurrence of higher-order scattering processes.^{45,47} In contrast, the sharper peaks near 305 and 715 cm^{-1} disappear completely at T_C for such single crystals, suggesting that their presence indicates a statically and tetragonally distorted structure.

Referring to the work of Perry and Hall, the reported Raman spectra for the tetragonal and orthorhombic phases of BaTiO_3 are similar.³³ All of the peaks observed for polydomain single crystals in the tetragonal phase appear also in the orthorhombic phase, and several of the peaks drift through 10's of wave number in the temperature range of stability for these phases. Subtle differences in the Raman spectra between the two phases relate to features in the $180\text{--}195\text{ cm}^{-1}$ range for powder and polydomain specimens. A positive intensity Raman peak at 180 cm^{-1} can be observed for single-domain single crystals of tetragonal BaTiO_3 when the appropriate crystal orientation is chosen. For other orientations, and often for powder specimens, a negative intensity peak is observed near $180\text{--}185\text{ cm}^{-1}$. This feature is proposed to be the result of interference between Raman-scattered radiation from two different modes, as explained by Robins *et al.*⁴⁵ In contrast, for the orthorhombic phase, a positive peak placed at $193\text{--}195\text{ cm}^{-1}$ has been readily observed for polydomain single crystals by Perry and Hall, as well as by Laabidi,

TABLE I. Summary of XRD, carbon analysis, and Raman-scattering data.

Proc. temp.	XRD structure	Carbon (wt %)	ν_1 (cm ⁻¹)	ν_2 (cm ⁻¹)	ν_3 (cm ⁻¹)	ν_4 (cm ⁻¹)	ν_5 (cm ⁻¹)	ν_6 (cm ⁻¹)	ν_7 (cm ⁻¹)
150 °C	Cubic	2.45							
400 °C	Cubic	0.81	183			525	722	805	1060
500 °C	Cubic	0.65	187			523	723	805	1060
600 °C	Cubic	0.33	189		303	517	721	805	1060
700 °C	Cubic	0.16	191	248	305	517	719		
800 °C	Cubic	0.10		252	307	519	715		
1000 °C	Tetragonal	0.06		252	307	519	715		
1200 °C	Tetragonal	0.03		252	306	519	719		
1350 °C	Tetragonal	0.02		242	307	515	718		

Fontana, and Jannot.^{33,48} In the spectra of Fig. 4, and for processing temperatures greater than 300 °C, the broad and sharper features of the Raman spectrum of tetragonal BaTiO₃ are both present. But, also clearly present for materials processed below 1000 °C is a positive intensity peak gradually increasing in wave number to 191 cm⁻¹ for 800 °C-treated BaTiO₃ (arrow), suggesting that a local orthorhombic, rather than tetragonal, structure exists for that material. Perry and Hall saw no shift in the placement of the peak from 195 cm⁻¹ over the temperature range of stability for the orthorhombic phase for their single crystal.³³

For materials showing the onset of a tetragonal distortion by XRD ($T_{\text{proc}} \geq 1000$ °C), the Raman spectra do not show the positive feature at all in the 180–200 cm⁻¹ range. Rather, for the 1350 °C-processed material, the negative peak at 180 cm⁻¹ is observed. These results suggest that the local crystal symmetry at the onset of global transformation detectable by XRD is tetragonal. For the room-temperature apparent transformation from the pseudocubic to the tetragonal structure for BaTiO₃ materials of grain size increasing from the nano scale, the local structure appears to evolve from orthorhombic to tetragonal symmetry as reported by others, based on temperature- and grain-size-dependent dielectric constant measurements.^{4,49} Figure 5 gives results for SHG intensity measurements at room temperature for the same specimens examined by XRD and Raman scattering.

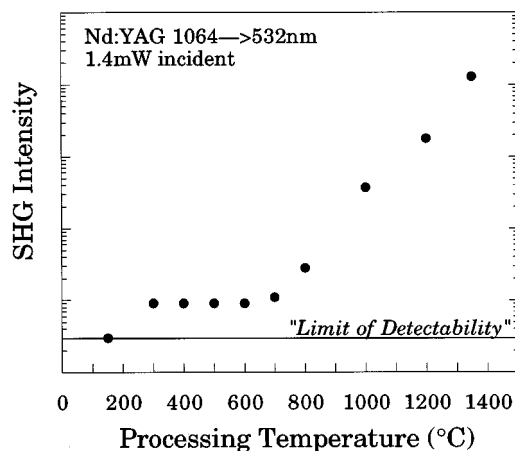


FIG. 5. Optical SHG intensity data recorded for BaTiO₃ xerogel pieces processed with increasing temperature.

These data suggest that the magnitude of the acentric distortions which exist for XRD-cubic BaTiO₃ are very small. Specifically, a measurable frequency-doubled signal was detected for the ultrafine material (grain size = 0.035 μm), but it was a factor of nearly 10³ weaker than that generated by the coarser grain (grain size ≈ 10 μm) BaTiO₃. Such a growth in SHG signal intensity with grain growth should not result from phase matching effects alone.³⁸ It should be noted that the bulk structure for the orthorhombic phase of BaTiO₃ is characterized by a spontaneous polarization of magnitude similar to that of the tetragonal phase.⁵⁰ Thus, the weak SHG signal for ultrafine grain specimens does not correlate with the reported bulk orthorhombic structure, but suggests the existence of a substantially suppressed lattice distortion. Referring to Figs. 2 and 5, significant growth in the SHG signal coincides with the development of a XRD-detectable tetragonal lattice distortion after heat treatment.

B. Hydroxyl defects

As was suggested to be likely for BaTiO₃ crystallized at very low temperature (< 150 °C) by the sol-gel method from alkoxide precursors, the presence of internal hydroxyl defects was verified in this study. Figure 6 gives IR spectroscopy data for a number of the specimens. As mentioned ear-

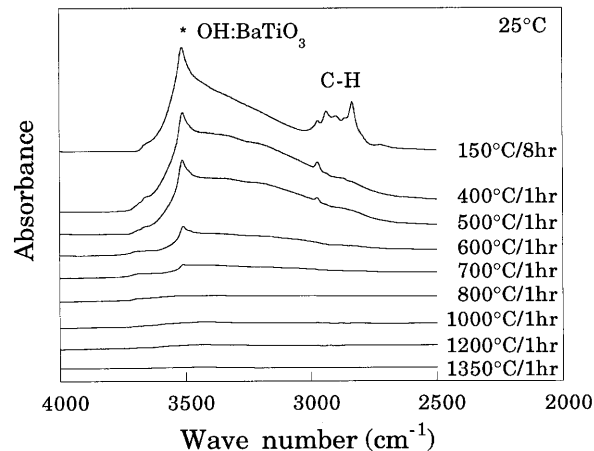


FIG. 6. Infrared spectroscopy data for alkoxide gel-derived BaTiO₃ illustrating the presence and liberation with heat treatment of hydroxyl defects.

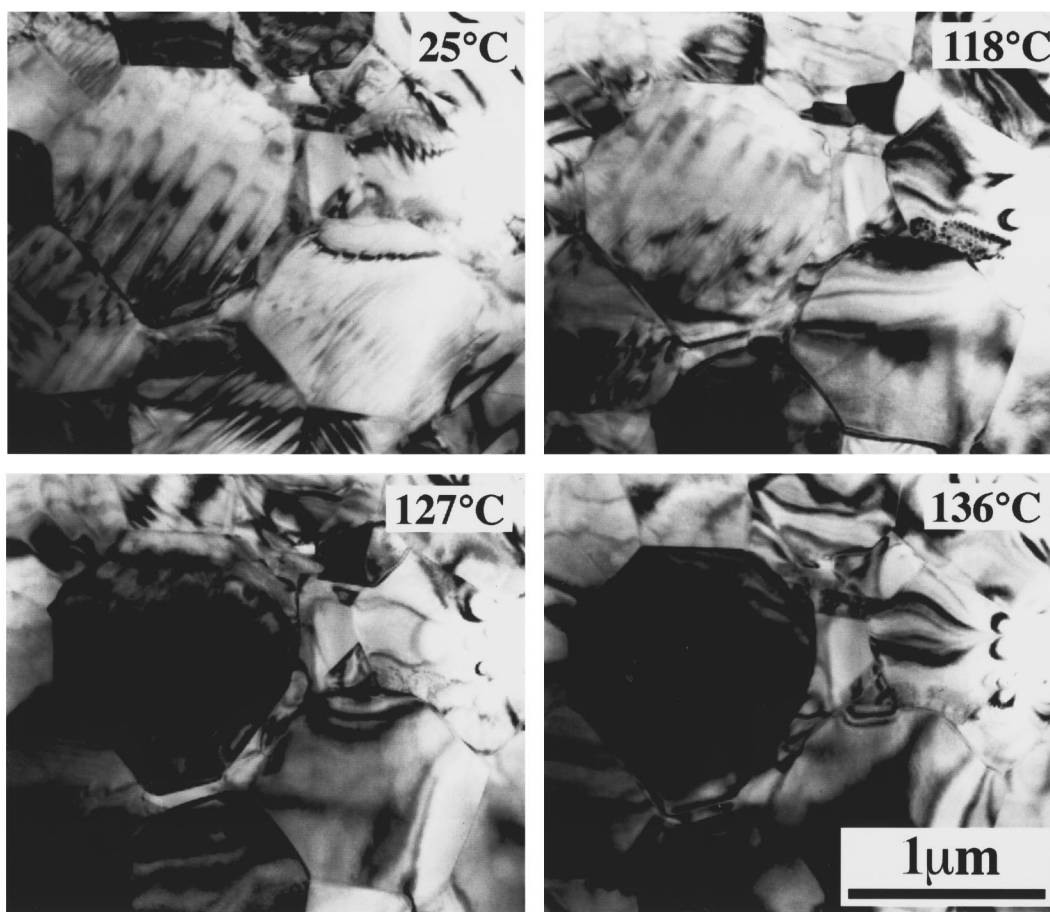


FIG. 7. TEM photomicrographs illustrating the development of a polydomain subgrain structure for BaTiO₃ of grain size 1 μm.

lier, several other authors have observed an absorption band near 3500 cm⁻¹ for hydrothermally grown BaTiO₃ powders and assigned it to the stretching mode of internal OH⁻ ions.^{10,29,30} This assignment is quite reasonable in light of spectra reported by others for single crystal BaTiO₃ intentionally prepared with hydroxyl defects.^{26–28} In the present work, the band was measured near 3510 cm⁻¹. Hydrogen defects are known to be very mobile in perovskites,²⁵ and we believe that this fact should be considered seriously when evaluating potentially useful insulators, in thin-layer form, processed by chemical methods at low temperatures; e.g., by hydrothermal growth or sol-gel deposition. Figures 1 and 6 taken together show that hydroxyl defects are annealed out long before the development of a global tetragonal structure for the heat treatment of sol-gel derived BaTiO₃. The defects were readily released by 800 °C, as shown in Fig. 6. Thus, the structure change detected by XRD after heat treatment at higher temperatures (1000 °C) appears not to be tied directly to the release of hydroxyls at 800 °C. Referring to Table I, we also conclude that the global symmetry change is not related to any marked or sudden elimination of carbon with heat treatment.

Figures 2 and 6 taken together show that a contraction of the pseudocubic lattice parameter coincides with the release of hydroxyls. Thus, while the hydroxyl content is not concluded here to be responsible entirely for the pseudocubic structure of ultrafine BaTiO₃, the defects are likely to strongly affect the measured pseudocubic lattice parameter.

Figures 1, 4, and 6 taken together reveal that XRD-cubic BaTiO₃, which is substantially free of hydroxyls, is Raman active (e.g., 800 °C-processed specimen). Thus, a lattice structure which is slightly distorted on some length scale exists for XRD-cubic materials either containing or free of hydroxyl defects. To summarize, hydroxyl defects were easily detected by IR spectroscopy. However, they appeared not to be associated directly with any changing structure characteristics with increasing heat-treatment temperature, except for the initial contraction of the lattice. We should point out that other defects associated with low-temperature processing would go undetected by this analysis, including nonstoichiometry, high vacancy concentrations, and extended line or planar defects. And, these defects could affect the stabilization of a long-range tetragonal structure.

C. Phase transformation behavior

A clear qualitative difference between the Raman spectra for partially ($T_{\text{proc}}=1000$ or 1200 °C) and fully ($T_{\text{proc}}=1350$ °C) tetragonal (by XRD) materials can also be seen in Fig. 4. SEM analysis placed the grain sizes at 0.1 and 0.4 μm, respectively, for the partially transformed materials. Referring to the work of Buessen, Cross, and Goswami, crystallites in such a microstructure would be expected to be nearly absent of 90° domains and in a stressed, incompletely transformed state.⁶ In contrast, the 10 μm grains of the 1350 °C sample should be freely twinned and transformed at

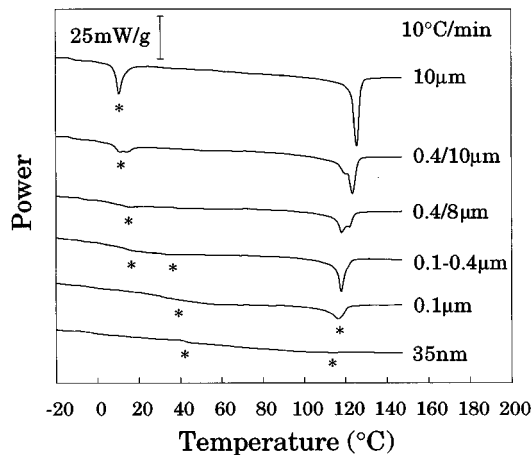


FIG. 8. DSC data for BaTiO₃ polycrystals, illustrating the dependence of phase transition thermal characteristics on grain size.

room temperature. We observe the fully realizable transformation strain in the XRD data of Fig. 1 and the negative Raman peak in Fig. 4 only for the larger grain size material. Figures 7(a)–7(d) illustrate the temperature dependence of the twinned subgrain structure for transformed BaTiO₃ of grain size 1 μm . Similar TEM analyses were carried out for grain sizes of 0.4, 0.1, and 0.035 μm . In agreement with the suggestion of Buessem, Cross, and Goswami, BaTiO₃ ceramics with decreasing grain size below 1 μm eventually became absent of transformation twins at room temperature.⁶ The 0.4 μm specimen showed twinning in some grains, while none could be observed for 0.1 and 0.035 μm grain sizes.

Figure 8 gives differential scanning calorimetry data recorded for BaTiO₃ polycrystals of various grain sizes. Endothermic features near 5 and 125 $^{\circ}\text{C}$ for larger grain specimens are attributable to the first-order orthorhombic-tetragonal and tetragonal-cubic transformations, respectively. Grain sizes are given in Fig. 8 from the previously described microstructure investigations of this report, and resulted from increasing processing temperatures from 800 to 1350 $^{\circ}\text{C}$. When two numbers are given, the microstructure had a bimodal grain size distribution, resulting from discontinuous grain growth. Clearly, there are marked changes which take place in the transformation behavior for materials with decreasing grain size. In particular, the tetragonal-cubic and orthorhombic-tetragonal transformations shift to lower and to higher temperatures, respectively, with decreasing grain size, as has been concluded previously based on dielectric constant data.^{4,49} It should be noted that the 0.1 μm grain-size specimen, which showed a broadened and shifted thermal anomaly associated with the cubic-tetragonal phase transformation, is the same which showed no twinning when characterized by hot-stage TEM. Thus, we propose this specimen exhibits single-domain behavior for individual grains. Eventually with decreasing grain size, the features associated with the two formerly independent transformations are lost in favor of a single very broad and weak feature. This anomaly characterizes materials which, at room-temperature, appear cubic to XRD and orthorhombic to Raman scattering. Values for the tetragonal-cubic transformation enthalpy ranged from 78 J/mol for the 0.1 μm grain

size to 183 J/mol for the 10 μm grain size. A value of 211 J/mol was measured for a top-seeded solution grown single crystal, which compares closely with reported values.⁵¹ A reduction in transformation enthalpy is reasonable for material exhibiting suppressed transformation characteristics (e.g., tetragonal distortion).

The thermal analysis and Raman-scattering data suggest that an enhanced stability exists for the orthorhombic structure when the grain size is reduced. This should be understandable in terms of the complex stress conditions within the grains of polycrystalline BaTiO₃ which is driven to undergo the ferroelectric transformation. Arlt described the strain fields which exist for a constrained grain which has twinned along {110} planes (90 $^{\circ}$ twinning) to minimize strain energy for a structural transformation of the BaTiO₃ cubic-tetragonal type.⁵ He reported a localized shear strain at grain boundaries, where the transformation was hindered. Since the unit cell of orthorhombic BaTiO₃ is characterized by a shear deformation of the cubic perovskite cell, it is understandable that BaTiO₃, with its ability to assume such a structure, would do so to some degree when under the influence of increasing shear stresses.

Thus, in order to understand the grain-size-dependent structure characteristics of BaTiO₃, a full assessment of the competition between constrained tetragonal and orthorhombic strain and twin boundary energetics must be developed. That is, enhanced stability for the orthorhombic phase, which appears to characterize ultrafine grain BaTiO₃, should be explainable in terms of its microstructure-constrained transformation strain energetics and its stress-relieving twinning mechanisms, as compared to the same for the tetragonal phase. For example, one should remember that the orthorhombic form of BaTiO₃ exhibits the capacity to polarize spontaneously along twice as many equivalent directions as does the tetragonal form. This fact alone would lead one to conclude that the orthorhombic form could more efficiently minimize transformation stresses, increasing its stability relative to the tetragonal phase.

With respect to the other possible causes for size effects which were discussed in the Introduction (i.e., loss of a long-range cooperative driving force and the action of a depolarization field), the following is concluded. Raman-scattering data clearly show that acentric distortions exist in ultrafine BaTiO₃ material. Thus, it is difficult to accept that the driving force for the ferroelectric transformation had been lost for very small grain size. While the full transformation strain is obviously not achieved for small crystallites, the Raman-scattering and SHG measurements suggest that some degree of acentricity exists. The possible action of a depolarization field is next considered. As discussed earlier, Batra and co-workers showed that for a given set of boundary conditions decreasing size resulted in instability of a polar phase.^{18–20} In the present work, specimens with grain size 0.1 μm and below are all single domain. And, the 0.1 μm grain size specimen is slightly transformed tetragonally, in terms of XRD and DSC measurements, while those of smaller grain size are not. However, it is the opinion of the authors that crystallites within a polycrystalline body should show substantial polarization compensation by charge transport and/or dipolar interaction between adjacent grains. Also, the evolution of phase transformation characteristics reported in this

paper do not agree with the behavior predicted for small BaTiO₃ particles under the influence of a depolarization field. Shih, Shih, and Aksay predicted a monotonic decrease in T_C through room temperature for particles with decreasing size below 0.5 μm .⁵² Thus, the depolarization effect is not believed to be highly influential in the presently studied specimens.

IV. CONCLUSIONS

(i) Hydroxyl defects were clearly observed by infrared spectroscopy for BaTiO₃ prepared by hydrolysis of alkoxide sol-gel precursors, and crystallized at very low temperature (< 150°C). The defects were liberated with heat treatment in air by 800°C.

(ii) Nanocrystalline BaTiO₃, which was cubic to XRD and free of hydroxyl defects, displayed Raman spectra attributable to the orthorhombic phase, and thermal analysis data supported the concept that grain-size reduction leads to enhanced stability of the orthorhombic phase at room temperature.

(iii) The Raman activity for XRD-cubic materials appears not to be associated only with the presence of internal hy-

droxyl defects, nor does the room-temperature structural transformation observed by XRD appear to be tied directly to their release. With increasing grain size from 0.035 to 0.1 μm , room-temperature XRD profiles and Raman spectra exhibited the characteristics of the tetragonal phase.

ACKNOWLEDGMENTS

This research was supported by the Basic Energy Sciences Division, U.S. Department of Energy under Grant No. DEFG02-91ER45439, the Fannie and John Hertz Foundation, the New Energy Development Organization of Japan, and an ISHM Educational Foundation Student Research Grant. We acknowledge the use of electron microscopy and x-ray diffraction facilities in the Center for Microanalysis of Materials, infrared spectrometers in the Center for Advanced Cement-Based Materials, and Raman-scattering equipment in the Beckman Institute. Elemental analysis was performed by the School of Chemical Sciences. The experimental assistance of Dr. Z. Xu with TEM, K. Stork with Raman scattering, K. Huggins with SHG characterization is gratefully acknowledged.

-
- ¹H. Kniepkamp and W. Heywang, *Z. Angew. Phys.* **6**, 385 (1954).
²D. A. G. Bruggeman, *Ann. Phys. (Paris)* **24**, 636 (1935).
³A. E. Jacobs, *Phys. Rev. B* **52**, 6327 (1995).
⁴G. Arlt, D. Hennings, and G. de With, *J. Appl. Phys.* **58**, 1619 (1985).
⁵G. Arlt, *Ferroelectrics* **104**, 217 (1990).
⁶W. R. Buessen, L. E. Cross, and A. K. Goswami, *J. Am. Ceram. Soc.* **49**, 33 (1966).
⁷M. H. Frey and D. A. Payne, *Appl. Phys. Lett.* **63**, 2753 (1993).
⁸S. Naka, F. Nakakita, Y. Suwa, and M. Inagaki, *Bull. Chem. Soc. Jpn.* **47**, 1168 (1974).
⁹K. Uchino, E. Sadanaga, and T. Hirose, *J. Am. Ceram. Soc.* **72**, 1555 (1989).
¹⁰D. Hennings and S. Schreinemacher, *J. Eur. Ceram. Soc.* **9**, 4 (1992).
¹¹B. D. Begg, E. R. Vance, and J. Nowotny, *J. Am. Ceram. Soc.* **77**, 3186 (1994).
¹²M. Criado, M. J. Dianez, F. Gotor, C. Real, M. Mundi, S. Ramos, and J. del Cerro, *Ferroelectric Lett.* **91**, 883 (1994).
¹³K. Ishikawa, K. Yoshikawa, and N. Okada, *Phys. Rev. B* **37**, 5852 (1988).
¹⁴W. L. Zhong, B. Jiang, P. L. Zhang, J. M. Ma, H. M. Cheng, Z. H. Yang, and L. X. Li, *J. Phys. Condens. Matter* **5**, 2619 (1993).
¹⁵S. Lu, H. Liu, Y. Han, L. Zhang, and X. Yao, *Ferroelectric Lett.* **18**, 115 (1994).
¹⁶P. Perriat, J. C. Niepce, and G. Caboche, *J. Therm. Anal.* **41**, 635 (1994).
¹⁷M. E. Lines and A. M. Glass, *Principles and Applications of Ferroelectrics and Related Materials* (Clarendon, Oxford, 1977).
¹⁸I. P. Batra, P. Wurfel, and B. D. Silverman, *Phys. Rev. Lett.* **30**, 384 (1973).
¹⁹I. P. Batra, P. Wurfel, and B. D. Silverman, *Phys. Rev. B* **8**, 3257 (1973).
²⁰P. Wurfel and I. P. Batra, *Phys. Rev. B* **8**, 5126 (1973).
²¹H. Ikawa, *Ceram. Trans.* **32**, 19 (1993).
²²R. E. Newnham, K. R. Udayakumar, and S. Trolier-McKinstry, in *Chemical Processing of Advanced Materials*, edited by L. L. Hench and J. K. West (Wiley, New York, 1992), p. 379.
²³L. L. Boyer, *Phys. Rev. B* **51**, 6201 (1995).
²⁴R. Waser, *J. Am. Ceram. Soc.* **71**, 58 (1988).
²⁵Yu. M. Baikov and E. K. Shalkova, *J. Solid State Chem.* **97**, 224 (1992).
²⁶I. Laulicht and L. Benguigui, *Solid State Commun.* **32**, 771 (1979).
²⁷S. Kapphan and G. Weber, *Ferroelectrics* **37**, 673 (1981).
²⁸A. Jovanović, M. Wöhlecke, S. Kapphan, A. Maillard, and G. Godefroy, *J. Phys. Chem. Solids* **50**, 632 (1989).
²⁹G. Busca, V. Buscaglia, M. Leoni, and P. Nanni, *Chem. Mater.* **6**, 955 (1994).
³⁰R. Vivekanandan and T. R. N. Kutty, *Powder Technol.* **57**, 181 (1989).
³¹B. D. Cullity, *The Elements of X-Ray Diffraction*, 2nd ed. (Addison-Wesley, Reading, MA, 1978).
³²*The Raman Effect*, edited by A. Anderson (Marcel Dekker, New York, 1973).
³³C. H. Perry and D. B. Hall, *Phys. Rev. Lett.* **15**, 700 (1965).
³⁴S. Schlag and H.-F. Eicke, *Solid State Commun.* **91**, 883 (1994).
³⁵S. Schlag, H.-F. Eicke, D. Mathys, and R. Guggenheim, *Langmuir* **10**, 3357 (1994).
³⁶M. H. Frey and D. A. Payne, *Chem. Mater.* **7**, 123 (1995).
³⁷J.-F. Campion, D. A. Payne, H. K. Chae, and Z. Xu, *Ceram. Trans.* **76**, 617 (1991).
³⁸S. K. Kurtz and T. T. Perry, *J. Appl. Phys.* **39**, 3798 (1968).
³⁹T. Takeuchi, K. Ado, T. Asai, H. Kageyama, Y. Saito, C. Masquelier, and O. Nakamura, *J. Am. Ceram. Soc.* **77**, 1665 (1994).
⁴⁰M. R. Leonard and A. Safari (unpublished).
⁴¹W. B. White, in *Infrared Spectra of Minerals*, edited by V. C.

- Farmer (Mineralogical Society, London, 1974), p. 242.
- ⁴²U. Balachandran and N. G. Eror, *J. Solid State Chem.* **42**, 276 (1982).
- ⁴³J. Javadpour and N. G. Eror, *J. Am. Ceram. Soc.* **71**, 206 (1988).
- ⁴⁴Ya. S. Bobovich, *Opt. Spectrosc.* **13**, 254 (1962).
- ⁴⁵L. H. Robins, D. L. Kaiser, L. D. Rotter, P. K. Schenck, G. T. Staaf, and D. Rytz, *J. Appl. Phys.* **76**, 7487 (1994).
- ⁴⁶A. M. Quittet and M. Lambert, *Solid State Commun.* **12**, 1053 (1973).
- ⁴⁷D. DiDomenico, Jr., S. H. Wemple, P. S. Porto, and R. P. Baum, *Phys. Rev.* **174**, 522 (1968).
- ⁴⁸K. Laabidi, M. D. Fontana, and B. Jannot, *Solid State Commun.* **76**, 765 (1990).
- ⁴⁹K. Kinoshita and A. Yamaji, *J. Appl. Phys.* **47**, 371 (1976).
- ⁵⁰G. H. Kwei, A. C. Lawson, S. J. L. Billinge, and S.-W. Cheong, *J. Phys. Chem.* **97**, 2368 (1993).
- ⁵¹G. Shirane and A. Takeda, in *Ferroelectrics and Related Substances; Oxides*, edited by K.-H. Hellwege, Landolt-Börnstein, New Series, Group X, Vol. 16a (Springer-Verlag, Berlin, 1981), p. 66.
- ⁵²W. Y. Shih, W.-H. Shih, and I. A. Aksay, *Phys. Rev. B* **50**, 15 575 (1994).